ISBN:0-08-042845-2 Published by Elsevier Science Ltd., 1998

SEISMIC PERFORMANCE OF MASONRY WALLS WITH BED JOINT REINFORCEMENT

A. E. Schultz[1], R. S. Hutchinson[1], and G. C. Cheok[2]

[1]Department of Civil Engineering, University of Minnesota
Minneapolis, MN 55455, USA
[2]Building and Fire Research Laboratory, National Institute of Standards and Technology
Gaithersburg, MD 20899, USA

ABSTRACT

In-plane cyclic load tests of partially grouted concrete masonry shear walls with bed joint reinforcement are presented. Specimen design and construction, and simulated seismic testing procedure are summarized. Lateral force resistance mechanisms are discussed in conjunction with observed displacement response. Parameters relating to initial stiffness, shear strength, energy dissipation and deformation capacity are highlighted, and initial stiffness predictions are compared with measurements.

INTRODUCTION

The development of seismic design procedures in the U.S. for masonry which is fully grouted and reinforced has been validated by experiment and observed performance during recent earthquakes. However, reinforced masonry has not gained widespread popularity in the eastern and central U.S. where seismic hazards are lower than those on the west coast. Cost-effectiveness and competition with other structural materials has often placed reinforced masonry at a disadvantage. In partially grouted masonry, vertical reinforcement is concentrated in fewer cells than in reinforced masonry, and only those vertical cells containing rebar are grouted. Horizontal bars are concentrated in bond beams, or they are replaced altogether by bed joint reinforcement. Large savings in construction costs are expected from partially grouted masonry (Fattal, 1993). Yet, the seismic resistance of partially grouted masonry must be quantified, and the applicability of current analysis and design methods for reinforced masonry needs verification.

A research project was initiated by the Building and Fire Research Laboratory (BFRL) of the National Institute of Standards and Technology (NIST) to study the seismic performance of partially grouted masonry shear walls (Fattal, 1993; Schultz, 1994). An experimental program was designed to determine the influence of horizontal reinforcement ratio, type of horizontal reinforcement and height-to-length aspect ratio on the shear strength and behavior of partially grouted masonry walls. This paper discusses the second of two series of partially grouted concrete masonry wall tests.

In the previous experimental study (Schultz, 1996a), six partially-grouted shear walls with bond beams containing deformed rebar were tested to determine seismic resistance characteristics. The study identified aspect ratio and amount of horizontal reinforcement as the primary variables. The data from the first series of tests demonstrated that partially-grouted masonry can have stable lateral resistance to seismic drift. The resistance mechanism was observed to differ from that for reinforced masonry walls, with vertical cracks arising from stress concentrations between ungrouted and grouted masonry dominating wall behavior. Height-to-length aspect ratio was found to have a beneficial effect on ultimate shear stress, but a detrimental one on toughness. Horizontal reinforcement ratio was found to have a modest but beneficial effect on ultimate shear stress, yet it did not appear to affect toughness.

In the present experimental study, horizontal reinforcement ratio (ρ_h) and height-to-length aspect ratio (H/L) are again the principal experimental variables, but welded wire grids (ladders) in the bed joints of the masonry provide all horizontal reinforcement. Porter and Braun (1997) have recently studied the strength characteristics of bed joint reinforcement in masonry walls, including bond and development. They have concluded that bed

Paper Reference: T119-4 (quote when citing this paper)

ISBN:0-08-042845-2 Published by Elsevier Science Ltd., 1998

joint reinforcement can serve to reinforce masonry walls as long as sufficiently large areas of horizontal reinforcement are provided. Thus, Porter and Braun (1997) provide experimental evidence in support of the analytical results reported by Schultz (1996b) regarding minimum horizontal reinforcement ratios in masonry shear walls. The present study represents full-scale shear wall tests to verify the applicability of bed joint reinforcement in partially grouted masonry walls.

EXPERIMENTAL PROGRAM

Six partially grouted masonry shear wall test specimens with bed joint reinforcement were constructed and tested (Table 1). An illustration of a typical specimen and the testing setup is given in Fig. 1. Only the outermost vertical cells of the walls were reinforced vertically and grouted, and the remainder of the masonry was ungrouted. Horizontal reinforcement was provided as welded wire grids (ladders) in the mortar bed joints between adjacent courses. All walls were built from seven courses of masonry for a total height of masonry equal to 1422 mm (56 in.), and all masonry courses were placed in a single day by an experienced mason. Exterior vertical cells were grouted on the following day. Wall lengths equal to 1422 mm (56 in.), 2032 mm (80 in.), and 2845 mm (112 in.) were used to define three different height-to-length aspect ratios (Fig. 2).

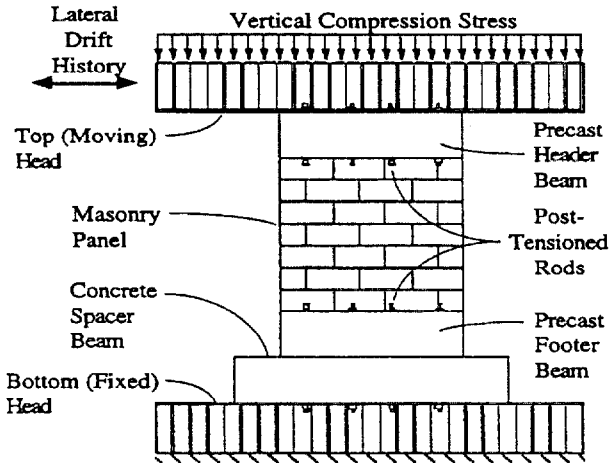

Fig. 1 Test setup and specimen configuration

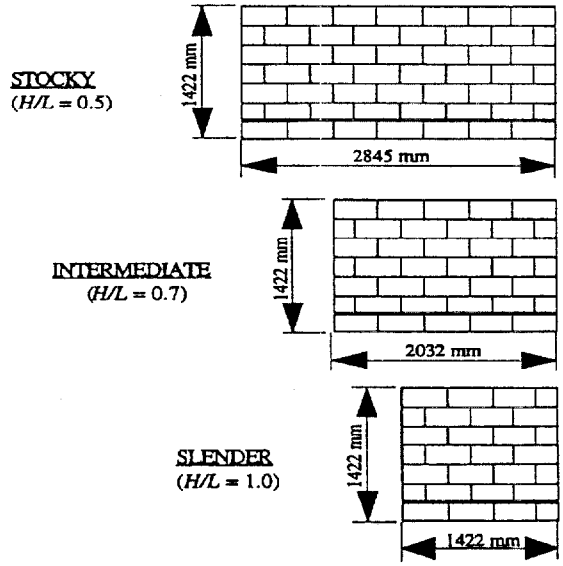

Fig. 2 Masonry panel configuration

TABLE 1
DETAILS OF SHEAR WALL SPECIMENS WITH BED JOINT REINFORCEMENT

Shear Wall No.	Specimen Designation	Length, mm (in.)	Aspect Ratio, H/L	Horizontal Reinforcement		Vertical Load, kN (kips)	
				Wire Gage	Ratio, ρ_h	Mean	Std. Dev.
2	CO-R05-J05-Q10	2845 (112)	0.5	No. 9	0.00056	265.0 (59.58)	11.3 (2.55)
4	CO-R07-J05-Q10	2032 (80)	0.7	No. 9	0.00056	185.4 (41.69)	8.4 (1.88)
6	CO-R10-J05-Q10	1422 (56)	1	No. 9	0.00056	130.2 (29.27)	5.9 (1.32)
8	CO-R05-J12-Q10	2845 (112)	0.5	No. 5	0.0011	265.5 (59.70)	4.9 (1.11)
10	CO-R07-J12-Q10	2032 (80)	0.7	No. 5	0.0011	187.6 (42.17)	5.6 (1.26)
12	CO-R10-J12-Q10	1422 (56)	1	No. 5	0.0011	133.2 (29.95)	4.5 (1.02)

ISBN:0-08-042845-2 Published by Elsevier Science Ltd., 1998

All six walls were reinforced with two #6 Grade 60 deformed bars in each exterior vertical cell, for a total area of vertical reinforcement equal to 1135 mm^2 (1.76 in.^{2}). This amount of reinforcement was deemed necessary to preclude flexural distress of the shear walls. Even though flexural yielding is a preferred response mode for seismic design, the purpose of this study requires that the specimens respond and fail in shear.

Bed joint reinforcement comprising welded wire grids in a "ladder" configuration were placed in all bed joints of all specimens, and two different wire sizes were used to fabricate the grids. Grids with No. 9 Gage longitudinal wires, the diameter of which is 3.76 mm (0.148 in.), were used for Wall Specimens 2, 4 and 6, while grids with No. 5 Gage longitudinal wire grids, which have a diameter equal to 5.26 mm (0.207 in.), were used for Wall Specimens 8, 10 and 12, to produce horizontal reinforcement ratios of 0.056% and 0.11%, respectively, based on gross dimensions (Table 1). The first of these ratios is slightly less than the minimum value cited in most building codes for masonry in the U.S. (MSJC, 1995; ICBO, 1997; NEHRP, 1995). In all grids, No. 9 Gage cross-wires were used, and in the interest of reducing overall grid thickness, the cross-wires were butt-welded to the longitudinal wires instead of lapped and welded, as is commonly done.

SPECIMEN CONSTRUCTION

The masonry walls were constructed using two-cell concrete blocks with average length, thickness and height equal to 396 mm (15.6 in.), 195 mm (7.67 in.) and 194 mm (7.63 in.), respectively. The units were 51% solid with a minimum face-shell thickness equal to 33.7 mm (1.33 in.). All masonry was face-shell bedded, except the exterior webs which were also bedded at the ends of the walls. The concrete block met the requirements for ASTM C90 (ASTM 1985), and the mortar was mixed using proportions that satisfy Type S in ASTM C270 (ASTM 1989). The grout mix for the exterior vertical cells was designed in accordance with ASTM C476 requirements for coarse grout (ASTM 1983). The 28-day compression tests for mortar and grout were 22.2 MPa (3220 psi) and 28.2 MPa (4090 psi), respectively, and the resulting masonry had 28-day compression strengths equal to 14.5 MPa (2100 psi) and 16.5 MPa (2390 psi), respectively, for ungrouted and grouted prisms. The concrete masonry units had a compression strength of 23.3 MPa (3380 psi).

The masonry panels were connected to precast concrete header and footer beams (Fig. 1) after the mortar hardened. Protruding ends of the vertical bars were inserted through sleeves into large pockets in the shape of a truncated pyramid in the header and footer beams, and the pockets were filled with high-strength grout. The vertical bars, the ends of which had been previously threaded, were anchored by means of steel plates and high-strength nuts. The bed joint reinforcing was placed such that either the cross wires or bent longitudinal wires engaged the vertical bars in the grouted cells. The bed joint reinforcement was specially manufactured for NIST by Baumann Research and Development Corp. (Newport Beach, CA), and the specifications included a minimum elongation of 6%, and for tensile test fractures to occur away from welded intersections.

TESTING PROCEDURE

The cyclic load tests were conducted in the NIST Tri-Directional Testing Facility (Woodward and Rankin 1989), as shown in Fig. 1. The header and footer beams, respectively, were attached to the upper and lower heads of the TTF by means of high-strength post-tensioned steel rods. In-plane cyclic drift histories were applied to the upper head while the lower head remained fixed. Since rotation of the header and footer beams was constrained, the panels were subjected to reverse bending. A response summary is given in Table 2.

TABLE 2
SUMMARY OF MEASURED SHEAR WALL RESPONSE

Shear Wall No.	First Major Event (FME)		Peak Load, kN (kips)	Peak Displacement, mm (in.)	Deformation Capacity	
	Load, kN (kips)	Displacement, mm (in.)			Displacement, mm (in.)	Drift Ratio (Δ/H)
2	197.8 (44.46)	1.6 (0.063)	261.3 (58.75)	18.2 (0.718)	17.6 (0.693)	0.0124
4	173.6 (39.02)	2.0 (0.080)	253.5 (56.99)	15.7 (0.618)	11.1 (0.436)	0.0078
6	97.6 (21.95)	2.2 (0.088)	175.9 (39.54)	15.4 (0.605)	12.2 (0.482)	0.0086
8	209.6 (47.12)	1.4 (0.054)	243.4 (54.71)	25.3 (0.995)	20.7 (0.814)	0.0145
10	174.4 (39.20)	1.7 (0.065)	270.3 (60.78)	17.9 (0.704)	12.5 (0.492)	0.0088
12	143.1 (32.18)	2.1 (0.081)	211.3 (47.51)	25.7 (1.011)	20.27 (0.798)	0.0143

ISBN:0-08-042845-2 Published by Elsevier Science Ltd., 1998

The cyclic drift histories were patterned after the TCCMAR phased-sequential displacement procedure (Porter and Tremel 1987). In this procedure, groups of drift cycles are organized around peak amplitudes that are gradually increased to failure. Peak amplitudes after the initial elastic displacements are tied to the first major event (FME) which can be interpreted as the first instance of significant damage. Because the TTF is essentially a displacement-controlled testing system, vertical loads were maintained only approximately constant during the tests (Table 1).

The first major event (FME) was defined as the first instance of visible crack formation observed during the test of each wall. This was the only technique that could be used to define the FME during testing, even though it is recognized that visible crack formation is not a very precise procedure since cracks may have formed prior to becoming visible and the masonry wall specimens were checked for cracks only at the peak displacement for each cycle. As a more precise verification of these measurements, the FME for each wall was equated with the proportional limits from smoothed force-displacement envelopes. The proportional limit was defined as the first marked departure from a nearly linear force-displacement relationship. A third way of establishing the FME comprised the identification of the first significant decrease in the lateral stiffness of a wall, and lateral stiffness was defined from the force-displacement envelopes as the ratio of lateral load to lateral displacement. Lateral loads at the FME for each wall obtained from the tests data using these three definitions were found to be in good agreement, consequently, only the force and displacement values at first visible cracking are listed in Table 2. It is worth noting that lateral load resistance at the FME decreases with increasing aspect ratio, but FME displacements appear to be independent of horizontal reinforcement ratio.

OBSERVED BEHAVIOR

Initial response to loading in the linear range exhibited very little outward evidence of damage. Invariably, the first observed instance of damage was the formation of vertical cracks in the top course near both jambs. The length of these cracks, when first noticed, varied from one-half of the height of a masonry unit to full unit height. The cracks were located at the interface between the grouted vertical cells and the adjacent ungrouted masonry, and they were almost undoubtedly the outcome of tensile stress concentration at the discontinuity. These stresses were generated by the horizontal loads applied to the top of the masonry panels.

It is of interest to note that in the previous series of tests in this program, i.e. the partially-grouted masonry shear walls with grouted bond beams (Schultz, 1996b), this kind of vertical cracking dominated response. After initial formation in the previous tests, the vertical cracks propagated downwards and traversed the anchorage regions of the bond beams. Thus, most stress transfer between the jambs and the rest of the masonry panels was interrupted. However, in the present series, no such domination of the jamb vertical cracks was observed. The specimens most affected by vertical cracking along the jambs were the stocky walls (Wall No. 2 and 8). But, even for these specimens, inclined cracking subsequent to the vertical cracks was noted in the upper one-half of the specimens. As the aspect ratio increased to $H/L = 0.7$ for Wall Specimens 4 and 10, more significant inclined cracking was noted. By the time aspect ratio H/L had reached a value of unity for Wall Specimens 6 and 12, inclined cracks with near 45° inclinations were observed. It is surmised that the bed joint reinforcement served to bridge the vertical cracks and prevented interruption of stress flow. Thus, the walls in the present series (i.e. with joint reinforcement) utilized the masonry more efficiently.

Multiple failures of the bed joint reinforcement by fracture were observed in all tests. However, these failures did not occur in close succession for a given wall. Rather, they took place throughout the portion of the tests characterized by large displacements. Furthermore, single fractures, or fractures of a few grid locations did not translate to measurable reductions in lateral force capacity.

FORCE - DISPLACEMENT RESPONSE

All six of the specimens with bed joint reinforcing responded to the cyclic drift histories in a stable manner (Fig. 3 and 4). The initial response was approximately linear and characterized by large stiffnesses. The force-displacement hysteresis curves widened as peak displacement increased, and "pinching" behavior (i.e. reduction in unloading stiffness at low lateral load levels) became more pronounced. It can be observed in Fig. 3 for a stocky wall ($H/L = 0.5$) and Fig. 4 for a slender wall ($H/L = 1$) that deterioration of post-peak strength and pinching of the hysteresis loops became more apparent with increasing height-to-length aspect ratio. The walls with the lowest aspect ratio (Wall Specimens 2 and 8) experienced a reduction in peak resistance of about 25%, followed by a stabilization and slight increase in resistance. The peak resistances of the other walls were marked by a gradual increase, followed by a more rapid post-peak decrease in load resistance. However, none of the walls failed suddenly, and all specimens were tested at least until the peak resistance for a given group of cycles dropped below 75% of maximum peak resistance.

Force-displacement envelopes were produced by collecting the force-displacement coordinate pairs for which displacement exceeded the previous maximum displacement (Fig. 5 and 6). Subsequently, an 11-point moving

ISBN:0-08-042845-2 Published by Elsevier Science Ltd., 1998

average was applied to the force history to "smooth" the envelopes. These envelopes indicate that the response of the wall specimens was linear during the early cycles and it became nonlinear after a certain point in the drift history (i.e. at the FME). The envelopes also show that, in general, the lateral resistance decreased as aspect ratio increased. However, this trend was not as apparent in the post-peak range. The envelopes illustrate the manner in which total lateral load resistance of the walls generally decreased with increasing aspect ratio (*H/L*). Furthermore, horizontal reinforcement ratio did not appear to have a significant effect on lateral load resistance, except for the slender walls. Wall Specimen 12 maintained a much higher lateral resistance than did Wall Specimen 6 throughout the cyclic drift history. In contrast, horizontal reinforcement ratio did appear to have a marked influence on the ability of the masonry to maintain peak load resistance at large drift demands.

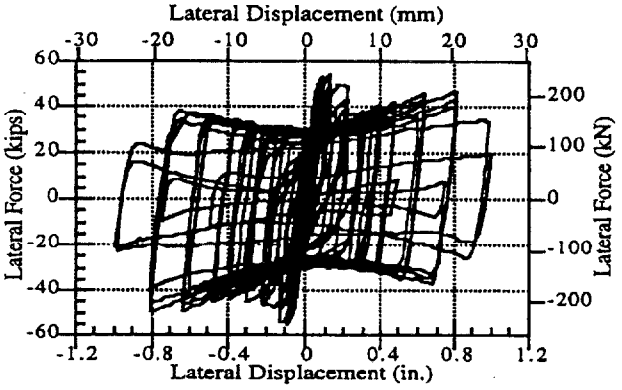

Fig. 3 Force-displacement response for Wall 8

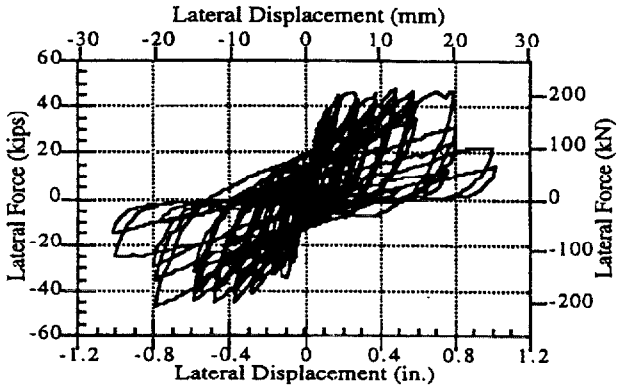

Fig. 4 Force-displacement response for Wall 12

Initial stiffnesses for each wall were inferred from the early cycles of the force-displacement histories, for which peak lateral force did not exceed 50% of the force at first cracking (i.e. at the FME). Lateral stiffness of the walls was based on these linear, elastic force-displacement cycles, and the stiffness was defined as the slope of the line connecting the positive and negative peaks of the force-displacement cycles. These inferred stiffnesses are listed in Table 3, along with estimates based on elastic behavior. Calculated stiffnesses were obtained using an estimated modulus of elasticity E_m equal to $750f'_m$, and the 28-day masonry compression strength for ungrouted prisms of 14.5 MPa (2100 psi) was used for f'_m. The shear modulus of elasticity was approximated as $0.4E_m$, and the panel thickness was taken to be twice the minimum face shell thickness. The stiffnesses of the walls were calculated by combining shear and flexural contributions, assuming that the walls were fixed at the base and restrained from rotation at the top. As noted in Table 3, aspect ratio (*H/L*) has a large impact on lateral stiffnesses. Also, calculated stiffnesses are in good agreement with the inferred quantities, and ratios of calculated to inferred stiffnesses range from 0.87 to 1.12 with a mean value of 0.99.

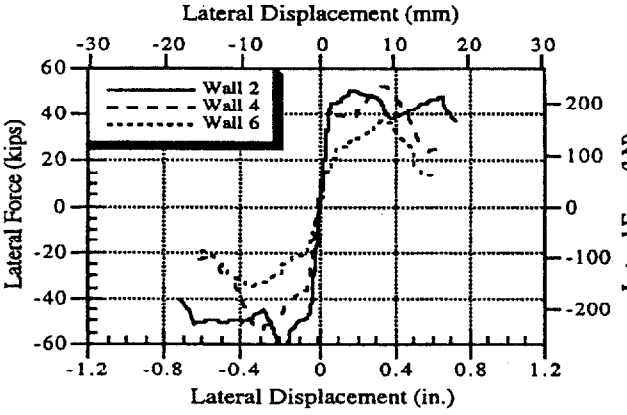

Fig. 5 Response envelopes for ρ_h=0.056%

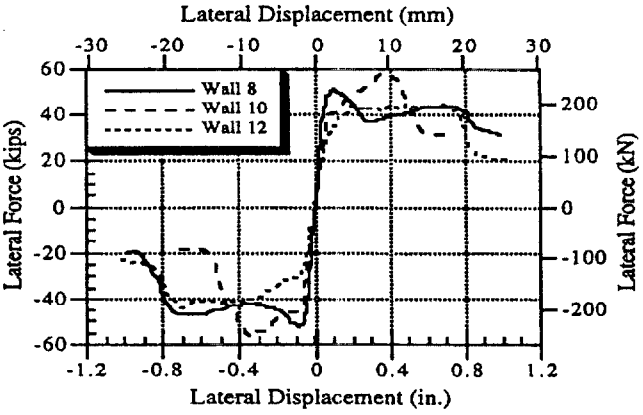

Fig. 6 Response envelopes for ρ_h=0.11%

ISBN:0-08-042845-2 Published by Elsevier Science Ltd., 1998

TABLE 3
INITIAL STIFFNESSES AND ENERGY DISSIPATION INDICES

Shear Wall No.	Initial Stiffness, kN/mm (kip/in.)		Inferred-to-Calculated Stiffness Ratio	Energy Dissipation Index		
	Inferred	Calculated		@Δ/H = 0.5%	@Δ/H = 1%	@Δ_{max}
2	501.5 (2864)	451.5 (2578)	1.111	65	281	311
4	265.8 (1518)	300.3 (1715)	0.885	70	132	137
6	158.8 (907)	183.3 (1047)	0.866	68	134	135
8	481.9 (2752)	451.5 (2578)	1.067	47	251	533
10	276.7 (1580)	300.3 (1715)	0.921	46	149	156
12	205.1 (1171)	183.3 (1047)	1.118	26	98	191

WALL TOUGHNESS

Two means of measuring the toughness of a wall are the ability to dissipate energy and the deformation capacity. Cumulative energy dissipation was evaluated by integrating each cycle of the force-displacement history and accumulating these areas. These values were then normalized by one-half the product of the force and displacement at the FME to account for the varying strengths and stiffnesses of the walls. Cumulative energy dissipation indices at the end of each cycle were paired with the current maximum displacement to define an energy dissipation-peak displacement relation. Cumulative energy dissipation indices are given in Table 3 at lateral displacements equal to 0.5% and 1.0% of wall height and at maximum displacement for each shear wall specimen. In relation to the energy dissipation indices at drift ratios of 0.5% and 1%, it appears that increasing the aspect ratio decreases the ability for the wall to dissipate energy, and horizontal reinforcement ratio has no significant effect on energy dissipation capacity. The energy dissipation indices at peak displacement (@Δ_{max}) for the walls with ρ_h = 0.11% (Wall No. 8, 10, and 12) greatly exceed those for the walls with ρ_h = 0.056% (Wall No. 2, 4 and 6), because the former had larger deformation capacities than the latter and were loaded over more cycles of displacement history.

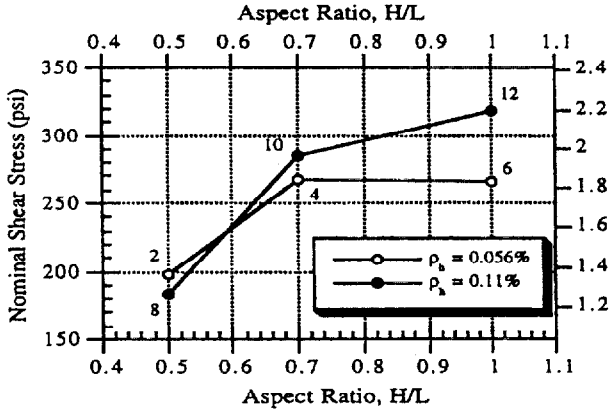

Fig. 7 Average ultimate shear stress vs. aspect ratio

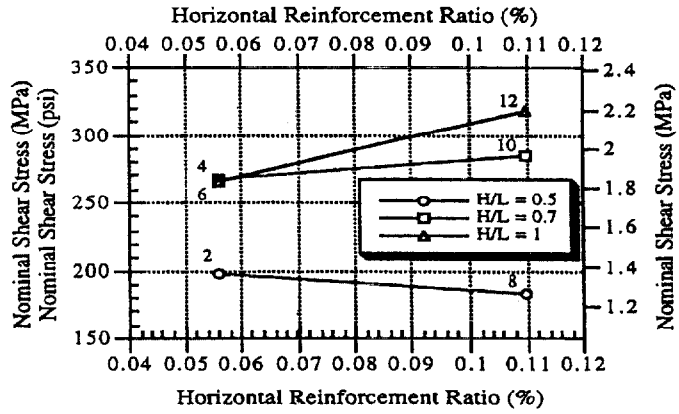

Fig. 8 Average ultimate shear stress vs. reinf. ratio

The deformation capacities were obtained from the force-displacement envelopes by determining the displacement at which lateral load capacity decreased permanently to less than 75% of the maximum load registered for a given wall in a given loading direction. These lateral displacements and the corresponding drift ratios are given in Table 2. Wall No. 2 and 8 are seen to undergo reductions in lateral load capacity below 75% of the peak load early in the tests, only to exceed the 75% margin at larger displacements. Consequently, deformation capacity was not deemed to have been attained until the load resistance of the walls dropped permanently below 75% of the peak capacity (Fig. 5 and 6). The deformation capacities shown in Table 2 exceed a drift ratio of 0.75%, and horizontal reinforcement ratio is seen to have a modest and consistent

ISBN:0-08-042845-2 Published by Elsevier Science Ltd., 1998

beneficial effect on deformation capacity: Increases in deformation capacity of 17, 13 and 66% were obtained, respectively, for walls with aspect ratios of 0.5, 0.7, and 1 as ρ_h was increased from 0.056 to 0.11%.

INFLUENCE OF EXPERIMENTAL PARAMETERS

Ultimate shear stresses were calculated for each wall specimen by dividing the average peak lateral load (Table 2) by net horizontal area. This net horizontal area was taken to be the product of twice the minimum face shell thickness of 33.8 mm (1.33 in.) and total wall length (Table 1). As shown in Fig. 7, ultimate shear stresses increased dramatically as aspect ratio increased from 0.5 to 0.7 (36% for walls with $\rho_h = 0.056\%$, and 55% for walls with $\rho_h = 0.11\%$). The aspect ratio increase from 0.7 to 1.0 indicates a smaller effect, i.e. -1% and 12%, respectively, for the lightly-reinforced and heavily-reinforced walls. The 0.056% to 0.11% increase in horizontal reinforcement ratio results in a more pronounced beneficial effect on the slender walls ($H/L = 1$), as ultimate shear stresses increase by 20% (Fig. 8). This increase is only 7% for walls with $H/L = 0.7$, and the ultimate shear stresses decrease by 7% for the stocky walls ($H/L = 0.5$).

CONCLUSIONS

The data presented in this paper suggests that partially-grouted masonry is a viable lateral-load resisting system for seismic design, and that bed joint reinforcement can serve as horizontal reinforcement provided that it meets minimum requirements regarding tensile behavior. Resistance of partially-grouted masonry shear walls to the seismic drift histories was found to be stable and featured high initial stiffness and ample energy dissipation. The lateral load resisting mechanism observed in the tests represents an improvement over that observed for the partially-grouted shear walls with bond beams in the previous experimental program. After initial formation of vertical cracks arising from stress concentrations between ungrouted and grouted masonry, the bed joint reinforcement was able to bridge the cracks and allow the masonry to continue carrying stress and form well-developed compression regions. Height-to-length aspect ratio was found to have a beneficial effect on ultimate shear stress, but a detrimental one on toughness (deformation and energy dissipation capacities). Horizontal reinforcement ratio was found to have a modest beneficial effect on ultimate shear stress and deformation capacity, but it did not affect energy dissipation. In addition, initial stiffnesses were estimated from masonry properties and first principles assuming an elastic panel.

REFERENCES

American Society for Testing and Materials (1983). *Standard Specification for Grout for Masonry.* ASTM C476-83, ASTM, Philadelphia, PA.

American Society for Testing and Materials (1985). *Standard Specification for Hollow Load-Bearing Concrete Masonry Units.* ASTM C90-85, ASTM, Philadelphia, PA.

American Society for Testing and Materials (1989). *Standard Specification for Mortar for Unit Masonry.* ASTM C270-89, ASTM, Philadelphia, PA.

Fattal, S. G., (1993). Research Plan for Masonry Shear Walls. *NISTIR 5117.* National Institute of Standards and Technology, Gaithersburg, MD.

International Conference of Building Officials (ICBO) (1997). *Uniform Building Code.* Whittier, CA.

Masonry Standards Joint Committee (MSJC) (1995). *Building Code Requirements for Masonry Structures.* ASCE 5-95, American Society of Civil Engineers, New York, NY.

National Earthquake Hazard Reduction Program (NEHRP) (1995). *Recommended Provisions for Seismic Regulations for New Buildings.* Part 1- Provisions. Part 2 - Commentary. FEMA 222A and 223A, Federal Emergency Management Agency, Washington, DC.

Porter, M. L. And Braun, R. L. (1997). Elemental Strength Tests of Joint Reinforcement in Masonry. Iowa State University, Department of Civil Engineering, Ames, IA.

Porter, M. L. and Tremel, P. M. (1987). Sequential Phased Displacement Procedure for TCCMAR Testing. Third Meeting of the Joint Technical Coordinating Committee on Masonry Research, US-Japan Coordinated Earthquake Research Program, Sapporo, Japan.

Schultz, A. E. (1994). NIST Research Program on the Seismic Resistance of Partially-Grouted Masonry Shear Walls. *NISTIR 5481.* National Institute of Standards and Technology, Gaithersburg, MD.

Schultz, A. E. (1996a). Seismic Resistance of Partially-Grouted Masonry Shear Walls. *Worldwide Advances in Structural Concrete and Masonry.* A. E. Schultz and S. L. McCabe (eds.) Proceedings of CCMS Symposium (ASCE Structures Congress XIV), ASCE, 211-222.

Schultz, A. E. (1996b). Minimum Horizontal Reinforcement Requirements for Seismic Design of Masonry Walls. *TMS Journal,* The Masonry Society, **14**(1), 49-64.

Woodward, K. and Rankin, F. (1984). The NBS Tri-Directional Test Facility. *NBSIR 84-2879.* National Bureau of Standards, Gaithersburg, MD.